

Production of a Design Developed for the Assembly Filter Parts, Optimization of Welding and Field Test

Hakan Maden^{1,*} – Kerim Çetinkaya²

¹ Ihlas Home Appliance, Turkey

² Antalya AKEV University, Faculty of Art and Design, Turkey

For the joining of non-removable plastic parts, methods such as friction welding, friction-stir welding, ultra-sonic welding, chemical joining, and hot-plate welding are used. Rotary friction welding is generally used for joining the filter parts of water treatment devices. After the rotating friction welding of the filter parts, semi-melted agglomerations are formed in the inner parts. To prevent semi-melted accumulation, a weld joint profile design was developed in the ABAQUS software in a previous study. In this study, injection moulds had been produced according to weld joint profile design. The taken plastic presses were welded with the friction welding machine and the joint was controlled and compared. It is seen that the semi-melted agglomeration was successfully confined. By performing Taguchi experimental method and ANOVA analysis on friction welding machine parameters, the optimum pressure conditions were determined in order to carry out static and dynamic tests according to NSF standards and field tests by producing 1500 pilot products, and it has been put into use. The lifetime of the developed filter depends on the material which was used in the manufacture. The next study is aimed to improve the lifetime of the developed filters.

Keywords: rotary friction welding, taguchi experimental method, ANOVA analysis, semi-melt agglomerations, NSF water purification, field test, static and dynamic testing

Highlights

- The friction-welded profiles of plastic parts have been developed to prevent semi-melt agglomeration stacking.
- Comparison of the developed friction-welded profile injection press was made.
- The Taguchi experimental method friction welding machine parameter has been applied.
- The friction welded parts were field-tested.

0 INTRODUCTION

The production stages of the plastic part are completed as design work, finite element method analysis (FEM), prototype production, mould-flow analysis, mould making, injection production, standard tests, and mass production. While the defects at the beginning can be corrected at a low cost in these stages, the cost increases as the stages progress. With FEM analysis, the structural defects in the part can be spotted before the material is produced and tested, which reduces the cost. After multiple verifications in the FEM process, the prototyping or moulding stage should be started; otherwise, the cost of correcting defects will be very high.

Parast et al. [1] 3D printed with acrylonitrile butadiene styrene (ABS) and polylactic acid (PLA) materials. ABS/ABS, PLA/PLA, and PLA/ABS were produced utilizing the rotary friction welding (RFW) process. Fatigue tests were performed on PLA and ABS samples. The findings revealed that PLA/PLA joints had superior fatigue resistance to non-welded PLA ones.

Cylindrical parts are made of AA1100 aluminium and H59 brass; combined with RFW. The RFW parameters were friction pressure of 90 MPa and

welding time of 15 seconds. They combined the H59 brass material with RFW by preheating (600 K and 873 K). The tensile strength of preheated and non-preheated parts was compared. They found that the part joined by RFW without preheating had a 33 % lower tensile strength (30 MPa) [2].

Bindal et al. [3] combined two polypropylene (PP) materials by using the RFW method. In this joining, they analysed the effects of welding pressure and rotating speed. The joining distance of surfaces reached a maximum value of 64.1 kPa in 14.2 mm at 1100 rpm. Sahu et al. [4] conducted an experimental study of 6 mm thick PP plates using the friction stir welding (FSW) method; they could not blend thermoplastic material with the conical pin. A square pin and the PP plates were successfully welded, according to welds they achieved 59.82 % maximum weld strength productivity. They observed that to obtain a high-strength weld, the assembly rotation and assembly process speed are effective.

Hamade et al. [5] joined the high intensity polyethylene (PE) material at 1224 rpm rotation speed, 40 feed rate, and maximum compressive force at 1085 N by RFW with 13.5 seconds of welding time in their study. They achieved the maximum temperature of

approximately 250 °C which is above the required melting temperature.

Kasman et al. [6] joined AA7075-T651 aluminium alloy plates by the FSW method with tools that had three different pin geometries and using two different rotational speeds; they compared the mechanical property of weld zone and microstructures.

In Saju and Velu's study [7], Inconel 718 and Nimonic 80A materials were joined by electron beam welding (EBW) and RFW methods. The metallurgical and mechanical properties of the joined parts were compared. The radiography test performed on both weld pieces revealed a weld defect. They found that the tensile strength of RFW welded joints was higher than that of EBW welded joints. In contrast, EBW welded joints exhibited higher ductility than RFW welds.

In conventional welding and friction welding (FW) methods, undesirable microstructures are formed due to high peak temperatures and cooling rates. Taysom and Sorensen [8] used different methods for slowing down the cooling and temperature control with the rotary friction welding method. Preheating was done before RFW, and then cooling was slowed down. They found that without temperature and cooling rate control, martensite forms easily after a weld. With temperature and cooling rate control, martensitic transformations are completely prevented, and a pearlitic microstructure has been observed.

Schmicker et al. [9] performed a simulation of RFW metal parts. They designed weld joint profile design and made simulations to trap the semi-melted material that formed in the inner part after welding.

Inline sediment and semi-melted accumulations in the inner part of the activated carbon filters cause premature clogging of the filters and low water flow. The weld joint profile structure was developed using the ABAQUS program to contain semi-melt accumulation. After the welding joint profile structure was developed, the plastic volume mould was revised, and prints were taken on the injection machine. Static and dynamic tests were carried out in accordance with National Sanitation Foundation (NSF) standards to measure the strength of the welded joint profile structure. Then, the Taguchi experimental method was applied to the parameters of the welding machine, and the optimum parameter values were determined. The field test was carried out by making pilot production according to the optimum parameter values determined.

1 SEMI-MELTED ACCUMULATION DEFECTS AFTER FW AND DEVELOPMENT OF WELDING JOINT PROFILE DESIGN

Due to the moulding and assembly errors of the plastic parts inside the sediment filter, the melt accumulation after FW closes the water passage channels in the filter upper cover part and narrows the water passage. While the supposed semi-melted accumulation situation occurs in Fig. 1a, the channels indicated by the red arrows in Fig. 1b cause water passages to be blocked as a result of defects. Post-production controls are made with air, and in these tests, a pass is given as long as there is no complete blockage in the channels. However, problems occur in water passages and low water flow or premature clogging of the filters during the installation at the customer's house

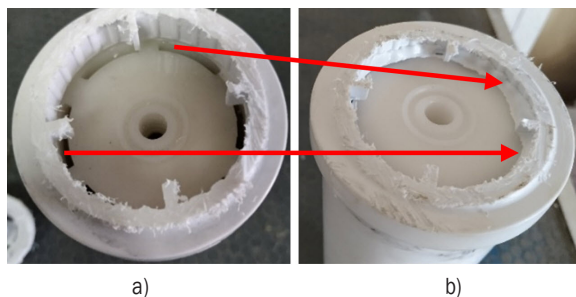


Fig. 1. a) Semi-melted agglomeration situation that should have been a sediment filter, and b) a semi-melted agglomeration situation with a faulty sediment filter

As a result of the fact that the activated carbon filter body part is small after the plastic injection press and the activated carbon bottom cover part is large after the plastic injection press, the lower cover part is jammed before it is seated on the base. In addition, the active carbon upper cover part cannot be fully seated in the slot due to faulty assembly by the personnel. Because of these, semi-melted agglomeration flows onto the felt in the top cover piece. Fig. 2a shows the semi-melted accumulation state of the activated carbon filter after welding. Due to the printing and assembly error that occurred, the semi-melted agglomeration indicated by the red arrow in Fig. 2b flows and fills the felt. The usage size of the felt, which is Ø60 mm, decreases to approximately Ø50 mm and 30 % is lost.

Fig. 3a shows a vectorial drawing of the currently used weld joint profile design. Fig. 3b shows the half-sectioned state of the existing filter after RFW and the vectorial drawing of the semi-melt agglomeration state. The semi-melted accumulation structure formed after FW was simulated in the ABAQUS program, and the semi-melt accumulation was obtained. Fig. 3c shows the semi-melt agglomeration result of the

ABAQUS analysis. It is seen that the semi-melted accumulation state indicated by the red arrow in Fig. 3 is similar to the structure formed on the piece and the structure made after the analysis.

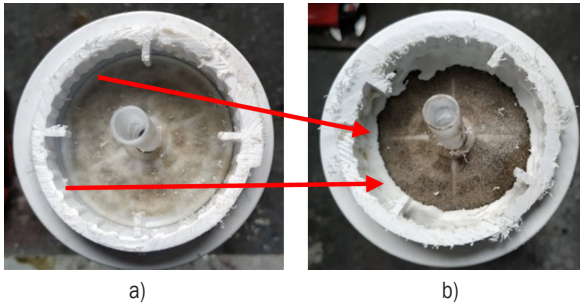


Fig. 2. a) Semi-melted agglomeration situation, which should be an activated carbon filter, and b) activated carbon filter faulty melt accumulation condition

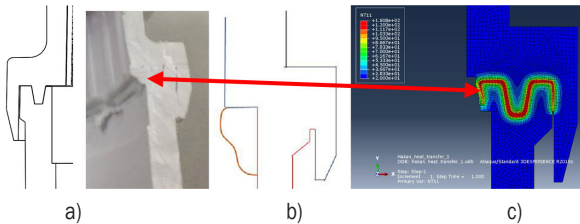


Fig. 3. Current part; a) weld joint profile design, b) the semi-melted agglomeration status, and c) the semi-melted agglomeration analysis [10]

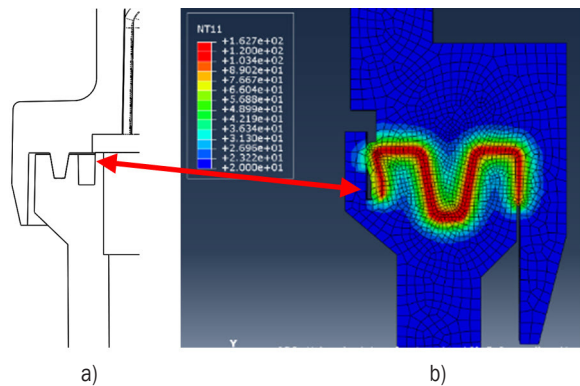


Fig. 4. a) Developed weld joint profile design, and b) the semi-melted agglomeration status analysis of the developed weld zone [10]

In the ABAQUS software, three different weld designs were made to contain the semi-melted accumulation, and the weld joint profile design was developed by making simulations of these weld joint profile designs. Fig. 4a shows the vectorial drawing of design no. 3 weld joint profile design. Fig. 4b shows the design developed weld joint profile design no. 3 and the semi-melted accumulation simulation made in the ABAQUS program [10]. As a result of the analysis

of the semi-melted accumulation, it is seen that the melt accumulation is successfully confined to the region indicated by the red arrow in Fig. 4.

2 THE MODIFICATION OF THE MOLDS IN ACCORDING TO DEVELOPED WELD JOINT PROFILE DESIGN

The design of the body and cover part of the filter of the developed welding joint profile design has been made. Moldflow analysis has been made to design parts to check defects as well as induction such as filling, merger marks and air voids [11]. Modifications have been made for the inline body and cover according to the designed part.

In Fig. 5, the inline body mould is seen. The existing inline body mould has been produced with four pores and inserts in the weld joint profile area. In the inline body mould's only pore, the inserts shown as A and B in Fig. 5 were manufactured and changed according to the developed design. Fig. 5 shows A, the change insert in the cavity side. Fig. 5 shows B, the changed insert on the core side.

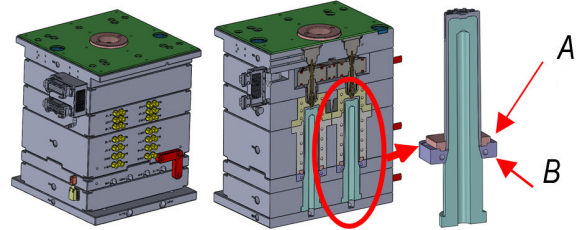


Fig. 5. Design of the inline body mould

In Fig. 6, the inline cover mould is seen. The existing inline cover mould has been produced with two pores and inserted in the weld joint profile area. In the inline cover mould only one pore and the six inserts shown as A, B, C, and D in Fig. 6 were manufactured and changed according to the developed design. Fig. 6 shows A, the dynamic Slide 1 piece, B, the dynamic Slide 2 piece, C, the inner core part, and D, the bottom support plate.

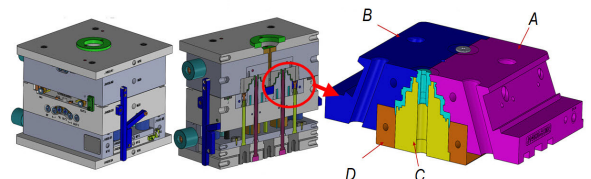


Fig. 6. Design of the inline cover mould

3 TAKING THE FIRST PRESS AND FRICTION WELDING

The mould insert parts, which were designed in accordance with the developed weld joint profile design, were manufactured and assembled. Then, the 20 parts in the first press were separated as junk in order to regulate the mould in the injection machine. After that, 300 pieces of inline body and cover parts have been pressed out. The parts pressed from the modified pore were separated, and the parts pressed from the other pore were sent for manufacturing. These parts will be used in the comprising analysis result and friction weld process, the determination of the optimum level of the welding machine, which is made with Taguchi experimental method and in the dynamic tests.

After the first press of the inline cover and body part, the design dimension and the other controls have been made. In the dimensional controls, it was seen that the difference between the design and the printed part was within the acceptable tolerance of DIN16901 [12]. The prints of the inline body and cover part are accepted.

Then, the consistency of the presses with each other us checked. In Fig. 7a, the first press of the inline body and cover can be seen in cut form. Fig. 7b shows the friction welding machine and the assembly of the parts. While the lower part is fixed in the friction welding machine, the upper part moves in both rotational and axial directions.

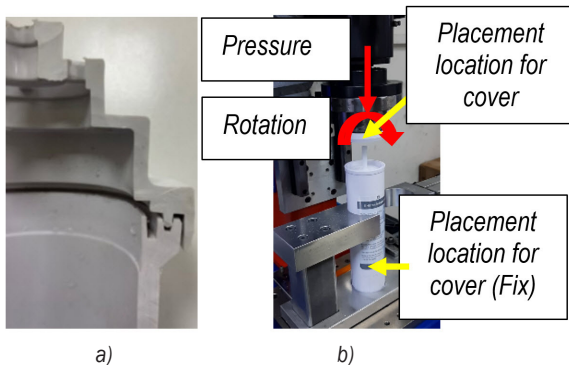


Fig. 7. a) First press of inline body and cover, and b) friction welding machine and part layout

Table 1. The values which entered the friction weld machine are shown

Input parameter name	Input parameter value
Rotation speed [rpm]	2490
Friction welding pressure [bar]	6
Friction welding duration [s]	2
Waiting time after friction welding [s]	3.5

The inline body cover piece has been joined with 10 pieces of 300 pressed-out pieces by a friction welding machine. The values used in the current production are entered as the welding machine parameter values. In Table 1, the values which entered our friction weld machine are shown.

In Fig. 8, the first press of the inline body and cover joined form are seen. It has been determined that there is no molten accumulation in the inner part of the 10 friction welds.

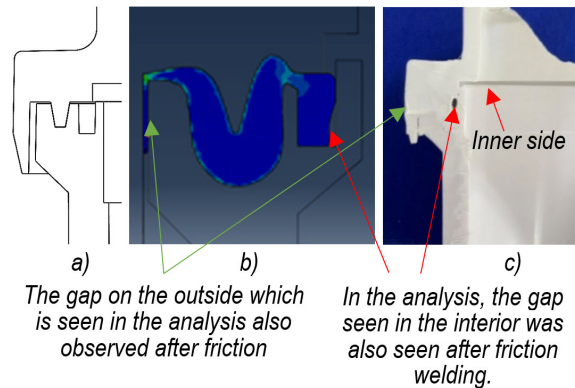


Fig. 8. a) The design of generally used welding joint profile, b) ABAQUS analysis of weld joint profile with developed design [10], and c) the status of the existing semi-melted accumulation after friction welding

The inline body and cover parts have been joined with the friction welding process. After the welding process, the cut view piece has been taken and whether there is semi-melted accumulation on the inner side is verified. In Fig. 8c, no semi-melted accumulation on the inner side has been observed. The semi-melted accumulation status acquired with ABAQUS software has been compared with the status of semi-melted accumulation after the welding process. It is observed that the semi-melted accumulation status is close to the structure acquired with the analysis result.

4 IMPLEMENTING TAGUCHI EXPERIMENTAL METHOD TO PARAMETERS OF FRICTION WELDING MACHINE

The Taguchi method is a well-developed experimental technique to determine the most optimum value range for a commonly used process. This method has a significant role in industry, when time and costs are very important. It is a helpful instrument for designing and developing high-quality systems. For these reasons, industries can significantly reduce product development time with the same cost by using the Taguchi method [13].

Van and Nguyen [14] combined AA6061 material by applying FSW. Welding machine parameters were developed by the Taguchi experimental method. The observed findings contributed significant data to determine optimal FSW parameters and enhance welding responses.

Singh et al. [15] combined the rotary friction welding process by adding aluminium and iron powder to plastic parts. Taguchi’s experimental method was applied to the data input parameters of the friction welding machine. They found that the parameters combination for the added aluminium powder to the plastic parts is 775 rpm 0.045 rotation per mm with 6 seconds welding time and for the added metal powder to the plastic parts is 1200 rpm, and 0.045 rotation per mm with 8 seconds welding time.

Özçelik [16] optimizes the effects of injection parameters and welding lines on the mechanical properties of PP moulding by using the Taguchi method and regression analysis. Park et al. [17] determined product thickness to prevent welding lines and also optimize the process condition by minimizing the induction press for the automotive fog lights’ blind cover.

A chiselling process has been made on a water-jet workbench in accordance with pressure advance rate and abrasive garnet amount of Anti-Proopiomelanocortin (POM-C). To determine the minimized surface roughness, the Taguchi experimental method was implemented. It was determined that on the water-jet workbench with 260 MPa pressure, 35 g/min garnet amount and 170 mm/min advance rate the surface roughness was the minimum rather than the other parameters [18].

The values of the FW machine are as important as the design of the welding structure on the joining quality of the inline body cover part. The Taguchi experimental method was applied to determine the optimum welding machine parameters.

5.1 Determination of Design Parameters

The effects of FW machine values such as rotation speed, friction welding pressure, friction welding time and waiting time on joint quality will be analysed. Minitab 15 [19] statistical software has been used to explain the effects of welding parameters and Taguchi experimental method analyses processes. The Taguchi method finds a solution by combining the three tools orthogonal experimental design, rate of signal/noise (S/N), and analysis of variance (ANOVA) to analyse and evaluate the numeric data [20] and [21].

In Table 2, the FW parameters and levels are shown. From these factors, the rotation speed level values were taken to be close to each other. If the speed is selected higher, it will cause the material to burn due to excessive friction in the weld area or the material structure will turn into an amorphous structure, causing an increase in brittleness. If the speed is selected low, there will not be a complete union because the heating in the weld area will not be excessive. Level values of other parameters were determined according to previous industry experience.

Table 2. The factors and levels of FW machine

Factors	Level 1	Level 2	Level 3	Level 4
Rotation speed [rpm] (A)	2310	2400	2490	2580
Friction welding pressure [bar] (B)	4	5	6	7
Friction welding duration [s] (C)	1.5	1.75	2	2.25
Cooldown time [s] (D)	2.5	3	3.5	4

Table 3. The tests will test according to Taguchi L16 orthogonal

Test number	Rotation speed (A)	Friction welding pressure (B)	Friction welding duration (C)	Cooldown time (D)
1	2310	4	1.5	2.5
2	2310	5	1.75	3
3	2310	6	2	3.5
4	2310	7	2.25	4
5	2400	4	1.75	3.5
6	2400	5	1.5	4
7	2400	6	2.25	2.5
8	2400	7	2	3
9	2490	4	2	4
10	2490	5	2.25	3.5
11	2490	6	1.5	3
12	2490	7	1.75	2.5
13	2580	4	2.25	3
14	2580	5	2	2.5
15	2580	6	1.75	4
16	2580	7	1.5	3.5

Four different level ranges (A, B, C, and D) were determined for four different parameters entered into the friction welding machine. If it is desired to perform experiments for each level shown in Table 2, 256 experiments from 4⁴ are required. With the Taguchi experimental method, it is possible to find the optimum value with 16 experiments. For these factors, the L16 4⁴ orthogonal index design was applied to be used in the Taguchi experimental design. After the determination of welding parameters, a Design of Experiments (DOE) has been generated from Taguchi’s experimental design and based on L16 4⁴

orthogonal matrix as shown in Table 3 [20] and [22] to [24].

The FW machine parameters have been set up as in Table 3 for the tests to be planned according to the L16 index. The machine has been run idle three times to calibrate parameter values. After that, three inline body and cover parts have been joined in accordance with determined parameters before for each of them with welding operation.

5.2 Determination of Durability of Combined Parts in the Parameters Determined According to the L16 Series

For the 16 different products that were welded with FW by considering the different levels of the factors in the experiments, the pressure tests have been made with a static pressure tool. The pressure was increased until each product exploded According to NSF/ANSI 58 5.1.3.2 hydraulic pressure test, in static pressure test value is 20.4 bar, in the dynamic pressure test for 5 seconds with 10.4 bar pressure and for 5 seconds without pressure, it is expected that 100,000 cycles are durable [25]. The pressure values here are accepted as the minimum value. These 16 different products have been tested until explode in the arbor press. In the static pressure test, the parts were tested in a transparent closed container.

The firm design has been developed by the signal-noise rate that was calculated from the values acquired from strategic computer simulation based on experimental design and used Taguchi method DOE orthogonal index [26].

S/N rate is a tool that statistically qualifies the Taguchi method’s performance characteristic and a logarithmic function of the requested answer that is defined as an objective function [20] and [27]. In this study, since obtaining the highest pressure values is desirable, the best and highest S/N ratios are used in the equality calculations.

$$S / N = -10 \cdot \log \left(\frac{1}{n} \cdot \sum_{i=1}^n \frac{1}{y_i^2} \right). \tag{1}$$

In Eq. (1), y_i is the observed data at the i^{th} experiment and n is the number of experiments.

For each test determined in accordance with Taguchi experimental method, which is in Table 4, three FW processes and for each part the static pressure test has been made at arbor press. For each test number, the average pressure test result made before has been acquired and the S/N value is calculated according to the average value. In Table 4, the strength test results and the S/N values calculated for Minitab 15 software are shown.



Fig. 9. Static test kit and the maximum pressure strength of 14/1 numbered test

Table 4. Tests’ strength and S/N values results

Test number	Rotation speed [rpm] (A)	Friction welding pressure [bar] (B)	Friction welding duration [s] (C)	Duration time [s] (D)	Strength [bar] (E)				S/N [dB]
					Test 1	Test 2	Test 3	Average	
1	2310	4	1.5	2.5	20.42	20.55	20.48	20.48	26.23
2	2310	5	1.75	3	23.73	23.45	23.53	23.57	27.45
3	2310	6	2	3.5	26.41	26.54	26.49	26.48	28.46
4	2310	7	2.25	4	25.86	26.08	26.12	26.02	28.31
5	2400	4	1.75	3.5	23.48	23.87	24.15	23.83	27.55
6	2400	5	1.5	4	24.35	24.67	24.52	24.51	27.79
7	2400	6	2.25	2.5	27.68	27.34	27.63	27.55	28.80
8	2400	7	2	3	27.14	27.32	27.36	27.27	28.72
9	2490	4	2	4	27.22	27.16	27.38	27.25	28.71
10	2490	5	2.25	3.5	28.05	28.41	28.33	28.26	29.03
11	2490	6	1.5	3	27.10	27.36	27.28	27.25	28.71
12	2490	7	1.75	2.5	27.89	27.64	27.75	27.76	28.87
13	2580	4	2.25	3	25.87	25.96	26.14	26.00	28.30
14	2580	5	2	2.5	27.58	27.44	27.62	27.55	28.80
15	2580	6	1.75	4	28.21	28.43	28.71	28.45	29.08
16	2580	7	1.5	3.5	26.32	26.54	26.78	26.54	28.48

In Fig. 9, the kit of arbor press where the static pressure test has been tested, the maximum value of 14/1 numbered combination's durability and the breaking point of the kit after the pressure test has been shown. After the friction welding process, a precise joint and residue of a piece have been observed. In the static pressure test, the wall thickness in the weld area is high, so the part bursts from the weak part. The results of the weld structure and part strength test, which were tested with 16 different tests, have been accepted because the test results are higher than the 20.4 bar static pressure value, which is the minimum standard value for NSF/ANSI 58 [25].

5.3 Optimum Induction Parameter Value and ANOVA

ANOVA a statically method used to determine the effects of two or more weld parameters [28]. In the case of determining the significance of the parameters which have effects on performance characteristics as statistical, ANOVA is used. Furthermore, to check the accuracy of test results acquired with the Taguchi method, lastly, a verification test is applied [20] and [21]. When the S/N rate of parameter levels are analysed, the most effective parameter on the strength are respectively rotation speed, the pressure of FW, friction duration and cooldown time has been observed. All factors are at optimal levels when the S/N response-ability is at the highest level [10].

Table 5. S/N response table of parameter levels

	Rotation speed (A)	Friction welding pressure (B)	Friction welding duration (C)	Cooldown time (D)
	S/N	S/N	S/N	S/N
Level 1	27.61	27.69	27.80	28.18
Level 2	28.21	28.27	28.24	28.29
Level 3	28.83	28.76	28.67	28.38
Level 4	28.66	28.59	28.61	28.47
Delta	1.22	1.07	0.87	0.30

Table 5 shows the S/N and strength values. The values are determined as the rotation is 2490 rpm,

Table 6. ANOVA analysis

Source	DF	Seq SS	Adj SS	Adj MS	F	P	Content ratio [%]
Rotation speed [rpm] A	3	3.565	3.565	1.18849	147	0.001	42.74
Friction welding pressure [bar] B	3	2.657	2.657	0.85563	110	0.001	31.85
Friction welding duration [s] C	3	1.929	1.929	0.64292	79.5	0.002	23.12
Cooldown time [s] D	3	0.19	0.19	0.06345	7.85	0.062	2.28
Error	3	0.024	0.024	0.00808			
Total	15	8.366					100

friction welding pressure is 6 bar, friction duration is 2 seconds and cooldown time is 4 seconds for the optimum level values (A3 B3 C3 D4) and friction welding verification part.

ANOVA analysis is necessary for commenting on the S/N values acquired with tests, ANOVA analysis enables seeing more clearly the effects of the results acquired in accordance with the used factors and their related levels on product strength [28]. In Table 6, the results of the ANOVA analysis are shown.

In ANOVA analysis, whether a parameter affects the response is determined by looking at the *P* (significance/probability) value. Considering the 95 % confidence interval, it concludes that the parameter affects the response when $P < 0.05$ (5 % significance value) [29]. Since the *P* value is above 0.05 in the ANOVA table (Table 6), the cooling time has no effect on the friction weld quality. In Table 8, the effects of each factor's percentage of contribution on total variation are shown at the rightmost. The most effective parameters for the strength of friction welding area rates are 42.74 % for rotation speed, 31.85 % for friction welding pressure and 23.12 % for friction welding duration has been observed. Also, the least effective parameter was determined as cooldown time with 2.28 % rate.

5.4 Forecast Calculation of the Best Choice

The strength gauge in the verification parts can in advance approximately calculated with mathematical in accordance with S/N ratio. Kahraman and Basar [30] found the optimum parameter for acquiring the lowest surface roughness on aluminium parts' boring process with the Taguchi experimental method. They have determined the value of surface roughness that can occur with optimum parameters by calculating with S/N rate. After, they observed that the two values are close, which are the calculated value and the value of surface roughness that occurs after the process with the optimum parameter value.

The estimated strength amount formula is as below.

$$F_t = (\max S / N_1 - N_m) + (\max S / N_2 - N_m) + (\max S / N_3 - N_m) + (\max S / N_4 - N_m), \quad (2)$$

where F_t is the sum of the differences between the selected best-levelled value of S/N and N_m , arithmetic average of S/N values for the calculated strength.

$$N_{hd} = F_t + N_m, \quad (3)$$

where N_{hd} is the calculated S/N rate for the test.

$$R_{day} = 10^{\frac{N_{hd}}{20}} \text{ [mm]}, \quad (4)$$

where R_{day} is the amount of maximum estimated strength.

It is envisioned that the estimated strength amount would be 30.014 bar when the estimating formula applies to joining strength analysis values of inline body and cover.

5.5 The Verification Test for Friction Welding Joining of the Inline Body and Cover Part

The optimum parameter values are determined with Taguchi experimental method. However, mass manufacturing should not be started in accordance with found optimum values. Before that, production should be produced in accordance with the determined optimum value and compared.

Taguchi's experimental method was applied to a DVD-ROM's front plastic cover to increase the bending strength and optimum values. They had 17.1% increase in the bending strength with the study of the front cover part [31].

Friction welding has been made to the body and cover parts in accordance with related test factors and levels for the verification test; five friction welding processes have been made to the parts. The bending strength values have been determined by applying the static pressure test to joined parts with friction welding. The determined strength and average strength values are shown in Table 7.

Table 7. The Table of average strength values for the verification part

Test 1 [bar]	Test 2 [bar]	Test 3 [bar]	Test 4 [bar]	Test 5 [bar]	Average strength [bar]
28.53	29.51	29.89	28.17	29.74	29.168

The average strength value for the parts joined with the friction welding process in accordance with

optimum parameters is determined as 29.168 bar. At the calculation, the strength value of the product emerged as 30.014 bar. The error rate between the validation test and the calculated value was 2.81%. In Fig. 12, the pressure value of test 1, which was produced with verification parameters, is shown. The test has shown that the side wall of the 1 numbered part exploded with cracked at the maximum strength in Fig. 10. It is observed that the joint area with friction welding resisted the pressure. In the static pressure test, the wall thickness in the weld area is high, so the part bursts from the weak part.



Fig. 10. The measurement of the verification part test 1

In Table 8, the calculated and measured strength values are shown.

Table 8. The comparison between the value of verification part and calculated value

The chosen parameter	Estimated calculated value [bar]	The average value of verification part [bar]
A3 B3 C3 D4	30.014	29.168

R_{day} with the implemented Taguchi experimental method, the friction welding parameters have been optimized. The acquired optimum level values (A3 B3 C3 D4) for the friction welding verification part were determined as 41.5 rps for rotation speed, 6 bar for friction welding pressure, 2 seconds for friction duration and 4 seconds for cooldown time. The average strength value for the part was made in accordance with friction welding optimum weld parameters acquired as 29.168 bar. The strength of the verification part can be estimated and calculated with mathematical calculation in accordance with the S/N rate in advance. According to this calculation, the strength value of the part is calculated as 30.014 bar. It can be observed that the strength value calculated and acquired with optimum parameters values emerged close. The difference has been accepted due to the effect on the quality of welding would be very low.

5.6 The Testing of Dynamic Friction Welding on Inline Body and Cover's Part

The strength of the friction welding joint profile structure that we have developed is above the desired level at the static pressure tests. On the joining point, the strength of static pressure can be high, although the strength of dynamic pressure can be low. The dynamic pressure has been tested in accordance with International NSF/ANSI 58 standard. In this test, it is desired that the part can be able to maintain its function and there should be no deformation for 5 seconds (<10.4 bar) with pressure and during 5 seconds without pressure with 100,000 cycles [25]. The dynamic test experiment has been implemented to this part, which is joined with friction welding for this purpose. In Fig. 11, the implementation of a dynamic test to the part joined with friction welding is shown.



Fig. 11. The dynamic test

In Fig. 11, five friction welded products' statuses are shown while performing the dynamic test. Due to lack of pressure on the city water, by way of a pump, the pressure has been increased up to 10 bar. The maximum pressure on the system was measured at 11.61 bar. The dynamic test started with 8 hours per day and the test has been completed in approximately 35 days (7 weeks). At the end of the test, approximately 105,000 cycles were implemented; it was observed that there are no deformation on the part form and no water leakage.

Filter parts joined by the friction welding process have successfully passed the dynamic tests. By producing 1500 pilot products, friction welded filters can be used at the customer's house in different weather conditions and water network pressures. It is intended to test such water leakage, cracking in the weld area, deformity of the filters and whether the improvement is beneficial or not.

6 RESULT & DISCUSSION

In inline filters used from water purification devices, semi-melted accumulations occur in the inner and outer parts after friction welding. The semi-melted accumulations formed in the interior cause clogging, a decrease in flow rate and clogging after the narrowing of the surface area in the activated carbon felt. Schmicker et al. [9] performed friction welding simulations of metal parts by rotating them in the software program they developed. To prevent metal semi-melted accumulation in the interior, a joint profile design has been developed and simulations have been carried out. To prevent metal semi-melted accumulation in the interior, a joint design has been developed and simulations have been practiced.

A finite element analysis method (ABAQUS) of the weld joint profile design has been developed to solve this problem and confine the semi-melted agglomeration in the interior. In Fig. 12, the semi-melted conditions of the developed weld joint profile designs are shown as a result of the analysis. From these melt conditions, it was observed that the welding joint profile design N3 imprisoned the semi-melted agglomeration.

Schmicker et al. [9] imprisoned semi-melted agglomerations in their study. In the results of the analysis made on the developed weld joint profile design, semi-melted agglomeration is imprisoned. Friction welding is applied to the plastic parts printed after the modifications made in the injection moulds.

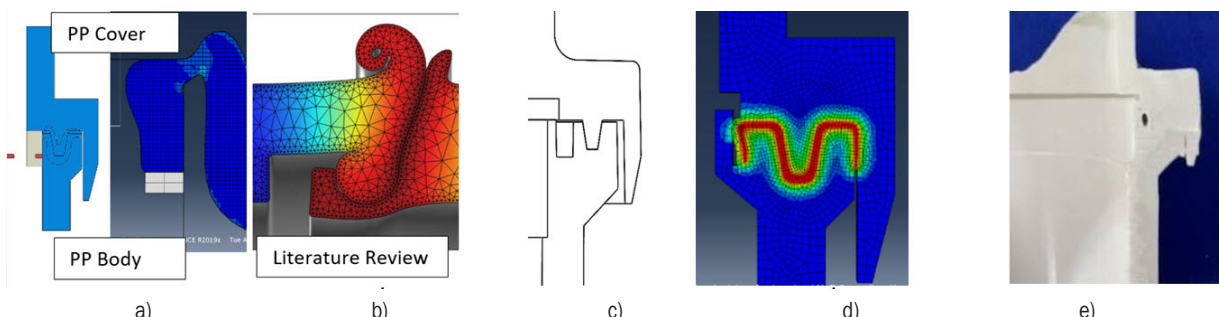


Fig. 12. a) Existing semi-melted accumulation analysis [10], b) literature search [9], c) developed weld joint profile design no. 3, d) melt accumulation analysis no. 3 design, and e) semi-melted agglomeration situation after friction welding

As a result of the analysis, a structure close to the semi-melted agglomeration was obtained and the semi-melted agglomeration was confined.

Filter parts joined by the FW process have successfully passed the static and dynamic tests according to NSF/ANSI 58, Chapter 5.1.3.2 standard [25]. By producing 1500 pilot products, friction welded filters can be used at the customer's house in different weather conditions and water network pressures. It is intended to test such water leakage, cracking in the weld area, deformity of the filters and whether the improvement is beneficial or not.

In the field test, 1500 already-existing manufactured products were sold, and 1500 new products produced with the design developed were followed up until the filter was changed after six months. Early replacement and defective filters were blocked from the filters in the following products. In Fig. 13, the semi-melted agglomeration status of the sediment filter is observed, and it is seen that there is no semi-melted agglomeration in the weld joint profile designed sediment filter and this result in reducing the failure rates.

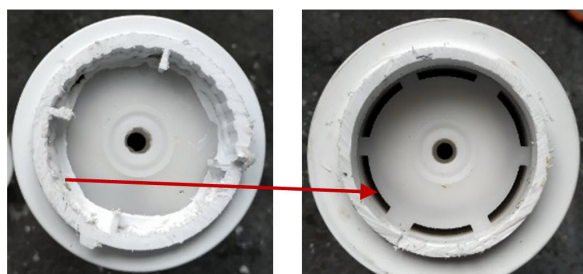


Fig. 13. a) Current manufacturing sediment filter, and b) weld joint profile developed sediment filter

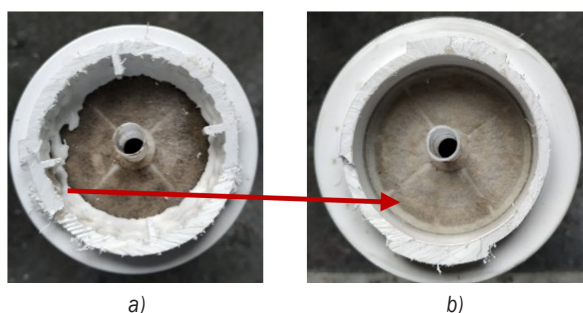


Fig. 14. a) Current manufacturing activated carbon filter, and b) weld joint profile developed activated carbon filter

In Fig. 14, the semi-melted accumulation state of the activated carbon filter is observed, and it is seen that there is no semi-melted accumulation on the surface of the felt in the activated carbon filter with a weld joint profile design. It is seen that the developed

weld joint profile design is beneficial for the activated carbon filter and reduces the failure rates.

In Fig. 15, enlarged pictures of the felt in the semi-melted agglomeration status of the activated carbon filter are shown. When the layered state of the felt is examined, particles larger than the pore diameter cause blockages. It prevents the passage of water.

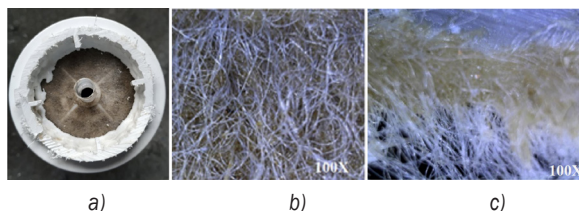


Fig. 15. a) Current manufacturing activated carbon filter, b) enlarged view of felt, and c) enlarged side section view of the felt

In Fig. 16, enlarged pictures of the felt in the weld joint profile developed activated carbon filter are shown. When the layered state of the felt is examined, there are few blockages in the pores. However, these blockages do not prevent the passage of water.

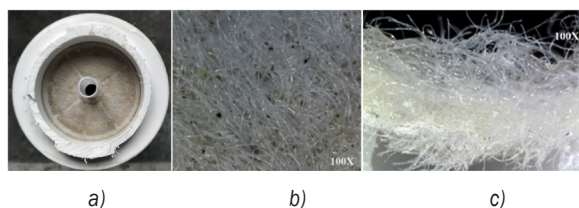


Fig. 16. a) Weld joint profile developed activated carbon filter, b) enlarged view of felt c) enlarged side section view of the felt

When the products from the field are examined, two sediment filters and one activated carbon filter are used in each product. For this reason, 3000 sediment filters and 1500 activated carbons were followed in 1500 products.

As can be seen in Table 9, the improvement in the friction weld joint profile structure reduced the error rates caused by semi-melted accumulation to zero. It has been determined that the filter changes do not decrease much depending on the quality of the water from the network.

7 CONCLUSIONS

In this study, moulds have been produced and product presses have been taken out according to the developed friction welding joint profile design. The values below have been acquired by implementing the

Table 9. Field test results of the filters produced

	Sediment filter - 3000 pieces						Activated carbon filter (GAC) - 1500 pieces			
	Semi-melted stacking clogging		Low flow as a result of semi-melted accumulation		Early filter change		Premature clogging of felt due to semi-melted stacking		Early filter change	
	Error amount	Error rate [%]	Error amount	Error rate [%]	Error amount	Error rate [%]	Error amount	Error rate [%]	Error amount	Error rate [%]
Developed weld joint profile design manufacturing	0	0.00	0	0.00	15	0.50	0	0.00	28	1.87
Current manufacturing	92	3.07	104	3.47	63	2.10	187	12.47	42	2.80

Taguchi experimental method and ANOVA analysis of friction welding machine parameters.

- The welding parameters for the friction welding area should be A3 B3 C3 D4 (rotation speed 2490 rpm, friction welding pressure 6 bar, friction welding duration 2 seconds, cooldown time 4 seconds) for the maximum strength;
- The rotation speed parameter has a 42.74 % rate effect on weld quality;
- The friction welding pressure parameter has a 31.85 % rate effect on weld quality;
- The cooldown time parameter has no effect on welding quality;
- The parts produced according to acquired optimum parameters' static and dynamic tests have been made in accordance with NSF standards, and no negative aspects have been observed
- At the implemented static pressure test, the average strength value is 29.168 bar, at the dynamic pressure test 5 seconds without pressure and 5 seconds with pressure at 11.6 bar there are 105,000 on/off (min 100,000 on/off). No negativity has been observed.

A field test was conducted to see whether the developed weld joint profile design is significantly improved. As field test results:

- It has been determined that the filter change rates caused by the semi-melted accumulation in the interior of the sediment filters are reduced to zero;
- It has been determined that the filter change rates caused by semi-melted accumulation in the inner part of the activated carbon filters are reduced to zero;
- it is now possible to manufacture inline membrane filters since there is no semi-melted accumulation in the interior.

REFERENCES

- [1] Parast, M.S.A., Bagheri, A., Kami, A., Azadi, M., Asghari, V. (2022) Bending fatigue behavior of fused filament fabrication 3D-printed ABS and PLA joints with rotary friction welding. *Progress in Additive Manufacturing*, DOI:10.1007/s40964-022-00307-5.
- [2] Halbin, G., Gulfeng, X., Jingcheng, L. Hao, L. (2022). Rotary friction welding of pure aluminum to preheated brass. *Welding in the World*, vol. 66, p. 2371-2376, DOI:10.1007/s40194-022-01367-5.
- [3] Bindal, T., Saxena, R.K., Pandey, S. (2020). Analysis of joint overlap during friction spin welding of plastics. *Materials Today: Proceedings*, vol. 26, p. 2798-2804, DOI:10.1016/j.matpr.2020.02.581.
- [4] Sahu, S.K., Mishra, D., Mahto, R.P., Sharma, V.M., Pal, S.K., Pal, K., Banerjee, S., Dash, P. (2018). Friction stir welding of polypropylene sheet. *Engineering Science and Technology, an International Journal*, vol. 21, no. 2, p. 245-254, DOI:10.1016/j.jestech.2018.03.002.
- [5] Hamade, R.F., Andari, T.R., Ammouri, A.H. Jawahir, I.S. (2019). Rotary friction welding versus fusion butt welding of plastic pipes - feasibility and energy perspective. *Procedia Manufacturing*, vol. 33, p. 693-700, DOI:10.1016/j.promfg.2019.04.087.
- [6] Kasman, Ş., Kahraman, F., Aydın, A. (2016). investigation of the effect of different stirrer pin geometries on welding performance of aa7075-t651 aluminum alloys joined by friction stir welding method. *International Symposium on Innovative Technologies in Engineering and Science*, p. 1393-1402.
- [7] Saju, T., Velu, M. (2022). Characterization of welded joints of dissimilar nickel-based superalloys by electron beam and rotary friction welding. *Journal of Materials Engineering and Performance*, DOI:10.1007/s11665-022-06958-3.
- [8] Taysom, B.S., Sorensen, C.D. (2020). Controlling martensite and pearlite formation with cooling rate and temperature control in rotary friction welding. *International Journal of Machine Tools & Manufacture*, vol. 150, art. ID 103512, DOI:10.1016/j.ijmachtools.2019.103512.
- [9] Schmicker, D. Persson, P.O., Strackelijan, J. (2014). Implicit geometry meshing for the simulation of rotary friction welding.

- Journal of Computational Physics*, vol. 270, p. 478-489, DOI:10.1016/j.jcp.2014.04.014.
- [10] Maden, H. and Çetinkaya, K. (2021). Joining analysis of polypropylene parts in rotary friction welding process and developing of joints profile. *Journal of Polytechnic*, vol. 24, no. 3, p. 1263-1273, DOI:10.2339/politeknik.824615.
- [11] Maden, H., Çetinkaya, K. (2020). Making moldflow analysis to produce different geometry parts in the same mold. *2nd International Scientific-Practical Conference: Modern Information. Measurement and Control Systems: Problems and Perspectives*.
- [12] DIN 16901 (1982). *Plastics Mouldings. Tolerances and acceptance conditions for linear dimensions*. from: <https://www.apm-mold.com/wp-content/uploads/2018/02/DIN-16901.pdf>, accessed on: 2022-06-25, Deutsches Institut für Normung, Berlin.
- [13] Taguchi, G. (1990). *Taguchi. Introduction to Quality Engineering*. Asian Productivity Organization. Tokyo.
- [14] Van, A.-L., Nguyen, T.-T. (2022). Optimization of friction stir welding operation using optimal taguchi-based ANFIS and genetic algorithm. *Strojniški vestnik - Journal of Mechanical Engineering*, vol. 68, no. 6, p. 424-438, DOI:10.5545/sv-jme.2022.111.
- [15] Singh, R., Kumar, R., Feo, L., Fraternali, F. (2016). Friction welding of dissimilar plastic/polymer materials with metal powder reinforcement for engineering applications. *Composites Part B: Engineering*, vol. 101, p. 77-89, DOI:10.1016/j.compositesb.2016.06.082.
- [16] Ozcelik, B. (2011). Optimization of injection parameters for mechanical properties of specimens with weld line of polypropylene using taguchi method. *International Communications in Heat and Mass Transfer*, vol. 38, no. 8, p. 1067-1072, DOI:10.1016/j.icheatmasstransfer.2011.04.025.
- [17] Park, C.H., Pyo, B.G., Choi, D.H., Koo, M.S. (2011). Design optimization of an automotive injection molded part for minimizing injection pressure and preventing weldlines. *Transaction Korean Soc Automotive Engineers*, vol. 19, no. 1, p. 66-72.
- [18] Altınsoy, A., Arslan, Y. (2021). Optimization of polyoxymethylene copolymer workability on water-jet machines using taguchi method. *International Journal of Eastern Anatolia Science Engineering and Design*, vol. 3, no. 1, p. 333-349.
- [19] Minitab 15. (2014). *User Manual Making Data Analysis Easier*. Minitab Inc. State College, San Francisco.
- [20] Phadke, M.S. (1989). Quality engineering using robust design. In Dehnad, K. (ed.) *Quality Control, Robust Design, and the Taguchi Method*. Springer, Boston, DOI:10.1007/978-1-4684-1472-1_3.
- [21] Yuin, W., Alan, W. (2000). *Taguchi Methods for Robust Design*. ASME Press, New York.
- [22] Fowlkes, W.Y., Creveling, C.M. (1995). *Engineering Methods for Robust Product Design: Using Taguchi Methods in Technology and Product Development*. Addison-Wesley Publishing Company, Boston, Massachusetts.
- [23] Schmidt, S.R., Creveling, C.M. (1997). *Understanding Industrial Designed Experiments*. Air Academy Press. Colorado.
- [24] Peace, G.S. (1992). *Taguchi Method: A Hands-On Approach*. Addison Wesley Publishing, Boston .
- [25] NSF/ANSI (2013). *Chapter 5.1.3.2, Hydrostatic pressure test - complete systems, NSF/ANSI 58 - 2013 Reverse Osmosis Drinking Water Treatment Systems*, p. 28; Michigan.
- [26] Park, S.H. (1996). *Robust Design and Analysis for Quality Engineering*. Chapman and Hall. London.
- [27] Ross, P.J. (1996). *Taguchi Techniques for Quality Engineering*. Mc Graw-Hill, New York.
- [28] Bilici, M.K., Bakır, B., Bozkurt, Y., Çalış, İ. (2016). Taguchi analysis of dissimilar aluminum sheets joined by friction stir spot welding. *Pamukkale University Journal of Engineering Sciences*, vol. 22, no. 1, p. 17-23, DOI:10.5505/pajes.2015.06641.
- [29] Savaşkan, M., Taptık, Y., Ürgen, M. (2004). Performance optimization of drill bits by experimental design method. *Istanbul Technical University Journal*, vol. 3, no. 6, p. 117-128.
- [30] Kahraman, F., Basar, G. (2018). The application of taguchi method in drilling process for optimization of multi response problem. *International Journal of Scientific and Technological Research*, vol. 4, no. 10, p. 1-9.
- [31] Öktem, H., Kır, D., Sarı, E.S., Çöl, M. (2018). Determination of the most appropriate injection process parameters affecting the mechanical properties of plastic products by Taguchi method. *Journal of Machine Design and Manufacturing*, vol. 14, no. 1, p. 8-16.